DOI: 10.1002/chem.200401236

A Combined ESI- and MALDI-MS(/MS) Study of Peripherally Persulfonylated Dendrimers: False Negative Results by MALDI-MS and Analysis of Defects**

Thorsten Felder,[a] Christoph A. Schalley,*[a] Hassan Fakhrnabavi,[a] and Oleg Lukin*[b]

Abstract: Mass spectrometry, in particular MALDI-MS, has often been used as a valuable means to characterize dendritic molecules with respect to their molecular masses. Also, it is a valuable tool for analyzing potential defects in their structure which result from incomplete synthetic steps. This article presents a comparison of ESI and MALDI mass spectrometric experiments on dendrimers persulfonylated at their periphery. While the ESI mass spectra easily permit impurities and defects to be identified and thus provide evidence for sample purity, reactions with acidic matrices occur during the MALDI process. The resulting defects are identical to those expected from incomplete substitution. Thus, in these cases, MALDI-MS yields false negative results. With mass-selected, ESI-generated ions, collision experiments were performed in an FT-ICR mass spectrometer cell to provide detailed insight into the fragmentation patterns of the various dendrimers. Different fragmentation patterns are observed depending on the exact structure of the dendrimer. Also, the nature of the charge is important. The fragmentation reactions for protonated species differ much from those binding a sodium or potassium ion. These differences can be traced back to different sites for binding H^+ versus Na^+ or K^+. Tandem MS experiments on mass-selected dendrimer ions with defects can be used to distinguish different types of defects. A concise structural assignment can thus be made on the basis of these experiments. Even mixtures of two isobaric defect variants with the same elemental composition can be identified.

Keywords: dendrimers · gas-phase reactions · mass spectrometry · matrix effects

Introduction

Dendrimer chemistry nicely illustrates that the development of a field of research depends much on the availability of suitable methods. When Buhleier, Wehner, and Vögtle published the first synthesis of what back in 1978 was coined "cascadanes",[1] unambiguous characterization of dendrimers with high masses was difficult. In principle, NMR experiments could help to identify the presence of structural defects, for example, through odd integrations, but the precision was not very high, especially for higher generations. Also, the exact nature of the defects was—and often still is—difficult to identify by NMR methods, because peaks are often broadened due to the large number of very similar building blocks located in different microenvironments. Mass spectrometry would have been the method of choice, but in 1978 none of the nowadays routinely used soft ionization techniques existed, with the exception of fast atom bombardment (FAB).[2] However, FAB is quite limited in the availability of a sufficiently large mass range and applicability to substances of low polarity. Consequently, it took almost a decade[3] for dendrimer chemistry to develop into a field of intense research.[4] Nowadays, matrix-assisted laser desorption/ionization (MALDI) mass spectrometry is considered to be a highly valuable tool for the characterization of dendrimers due to the large mass range of the mass analyzers usually coupled to the MALDI ion source.[5] Also, electrospray ionization (ESI) has been used to ionize den-

[a] Dipl.-Chem. T. Felder, Priv.-Doz. Dr. C. A. Schalley, Dipl.-Chem. H. Fakhrnabavi
Kekulé-Institut für Organische Chemie und Biochemie der Universität
Gerhard-Domagk-Strasse 1, 53121 Bonn (Germany)
Fax: (+49) 228-735-662
E-mail: c.schalley@uni-bonn.de

[b] Dr. O. Lukin
Institut für Polymere, Wolgang-Pauli-Str. 10
ETH Hönggerberg, HCI G 527, 8093 Zürich (Switzerland)
Fax: (+41) 446331397
E-mail: oleg.lukin@mat.ethz.ch

[**] ESI = electrospray ionization; MALDI = matrix-assisted laser desorption/ionization.

drimers and transfer them into the gas phase as intact species.[6] A central question for precise mass spectrometric characterization of dendrimers is whether additional signals below the molecular mass of the structurally perfect species are due to fragments formed during ionization or due to defects[7] originating from the synthesis. To distinguish between them, it is highly desirable to understand the fragmentation patterns of dendrimer ions in the gas phase, which can be unraveled by tandem mass spectrometric experiments (MS/MS).[8] Mass spectrometry may provide even more information, for example, on the site of protonation in the gas phase[9] as compared to solution, on the self-assembly of dendrimers,[10] and on weak, noncovalently bound host–guest complexes of dendritic species.[11] These results demonstrate the remarkable power of mass spectrometry for a detailed characterization of dendrimers, without which the fast pace of development in this field would not have been possible.

Here a detailed mass spectrometric study of a novel type of dendrimers is presented. These dendrimers are based on tris(2-aminoethyl)amine (TREN) and polypropyleneamino (POPAM) scaffolds that are persulfonylated at their periphery.[12] While their ESI mass spectra exhibit only a very small amount of defects and thus ascertain a high degree of purity, the MALDI mass spectra seemingly suggest the presence of large amounts of defect variants when acidic matrices are used. These findings are rationalized by reactions of the dendrimers with the matrix during the MALDI process which produce exactly those species which would result from incomplete substitution during synthesis. The possibility of false negative results from MALDI mass spectrometry is an important piece of information for the synthetic chemist. On the basis of the MALDI mass spectra, one might draw wrong conclusions on impurities in the samples that are actually not present at all. In addition, the fragmentation patterns of the dendrimers are examined in MS/MS experiments through collision-induced dissociation of the corresponding ions. We provide evidence that tandem MS experiments are capable of distinguishing the structure of defect variants through differences in their fragmentation patterns.

Abstract in German: *Massenspektrometrie, insbesondere MALDI-MS wurde oft als wertvolle Analysenmethode für die Charakterisierung von Dendrimeren hinsichtlich ihrer Molekülmasse, aber auch hinsichtlich einer Analyse potentieller Strukturdefekte eingesetzt, die aus unvollständig verlaufenden Synthesestufen resultieren. In diesem Artikel berichten wir über einen Vergleich von ESI- und MALDI-massenspektrometrischen Experimenten mit an ihrer Peripherie persulfonylierten Dendrimeren. Während die ESI-Massenspektren eine einfache Identifizierung von Verunreinigungen und Defekten erlauben und damit eine Reinheitskontrolle ermöglichen, laufen während der Ionisierung mittels MALDI Reaktionen mit sauren Matrices ab, die genau solche Defekte erzeugen, wie man sie aus einer unvollständigen Synthese erwarten würde. MALDI-MS führt hier also zu einem falschnegativen Ergebnis. Mit massenselektierten Ionen aus der Electrospray-Ionisierung wurden Stoßexperimente in einer FT-ICR-Zelle durchgeführt, um einen detaillierten Einblick in das Fragmentierungsmuster der verschiedenen Dendrimere zu erhalten. Man beobachtet unterschiedliche Fragmentierungsmuster in Abhängigkeit von der genauen Struktur der Dendrimere. Auch die Art der Ladung ist wichtig, da die Fragmentierungswege der protonierten Dendrimere sich deutlich von denen ihrer Na^+- und K^+-Addukte unterscheiden. Diese Unterschiede können auf unterschiedliche Bindungsstellen für H^+ gegenüber Na^+ oder K^+ zurückgeführt werden. Tandem MS-Experimente mit massenselektierten, strukturdefekten Dendrimer-Ionen erlauben eine genaue Unterscheidung verschiedener Typen von Defekten. Sie können daher für eine detaillierte Strukturaufklärung verwendet werden. Sogar Mischungen zweier isobarer Defektvarianten mit gleicher Elementarzusammensetzung werden zuverlässig identifiziert.*

Results and Discussion

First-generation TREN-based persulfonylated dendrimers: Comparison of ESI and MALDI mass spectra: Scheme 1 shows generation-1 (G1) dendrimers **1**–**3** and generation-2 (G2) dendrimers **4** and **5**, which are based on the TREN scaffold. They carry sulfonimide end groups that bear methoxyl, cyano, or alkyl substituents *para* to the sulfonyl groups. Since a stepwise synthetic procedure is feasible that involves formation of sulfonamides in the first step followed by conversion to sulfonimides in the second step, dendrimer **3** is functionalized with two different methoxy- and cyano-substituted arylsulfonyl groups, respectively, at each terminal branch. Their synthesis was reported earlier[12] and we therefore focus on the mass spectrometric characterization here.

When ionization is achieved by electrospray ionization (ESI) of 50 μM solutions of these dendrimers in methanol with 1 % acetic acid to facilitate protonation, these dendrimers give rather clean mass spectra (Figure 1a). It is easy to detect the quasimolecular ions of, for example, **1** at *m/z* 1167 and their accompanying sodium and potassium adducts at *m/z* 1189 and 1205, respectively. The isotope patterns obtained by experiment closely match those calculated on the basis of natural abundances. Minor additional signals for the sodium and potassium adducts of **6** are observed, which indicate that the sample contains a small amount of this defect as impurity. We were able to trace it back to the impurity of commercially available TREN. When the highest quality of TREN was used in the synthesis, this impurity was not observed. Consequently, the ESI-FT-ICR mass spectrum in Figure 1 provides excellent information on the purity of the dendrimer samples and permits defects to be identified.

However, the spectrum changes dramatically when matrix-assisted laser desorption/ionization (MALDI) was

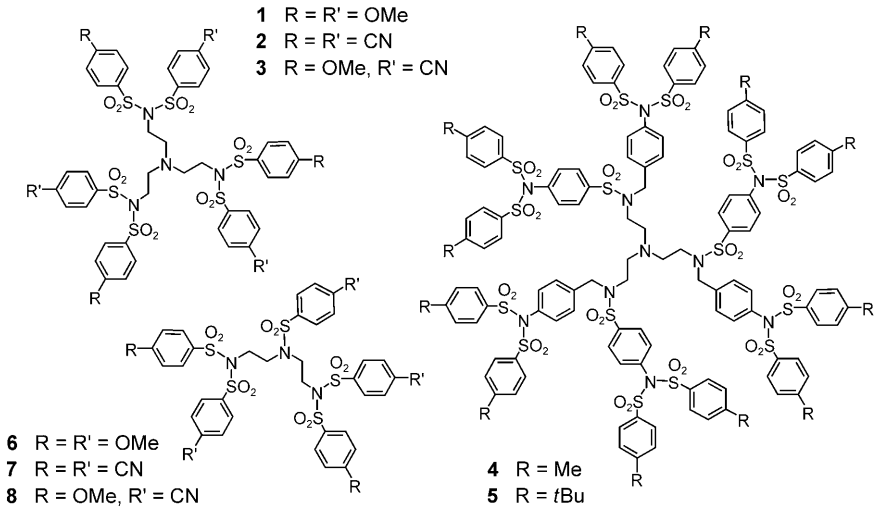

Scheme 1. Persulfonylated dendrimers **1**–**5** based on a TREN scaffold. Compounds **6**–**8** are impurities that were observed in the mass spectra when synthesis-grade TREN was used, which contains some bis(2-aminoethyl)amine.

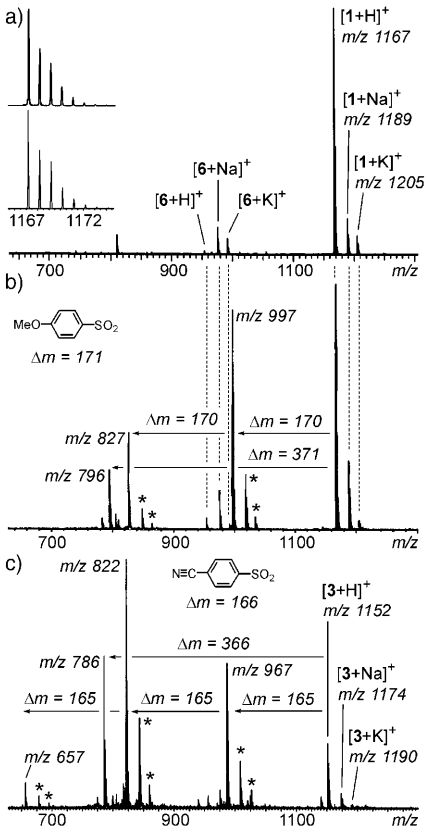

Figure 1. a) ESI-FT-ICR mass spectrum of a 50 μM methanol solution of dendrimer **1** containing about 1% acetic acid. Inset: Isotope pattern obtained by experiment (top) and calculated on the basis of natural isotope abundances (bottom). b) MALDI-TOF mass spectrum of **1** with 2,5-dihydroxybenzoic acid (DHB) as matrix. c) MALDI-TOF mass spectrum (DHB) of **3**. Asterisks denote Na^+ and K^+ adducts of the decomposition products.

used for the generation of ions from the dendrimer samples. The MALDI-TOF mass spectrum of the same sample of **1** which was used for the ESI mass spectrum discussed above is shown in Figure 1b. It shows the same signals that were observed in the ESI mass spectrum, but in addition quite intense signals are found at *m/z* 997 ($\Delta m = 170$), at 827 ($\Delta m = 340 = 2 \times 170$), and 796 ($\Delta m = 371$). Whereas the first two are accompanied by sodium and potassium adducts in roughly the same intensity ratios as the parent ion, no such adducts are found for the signal at *m/z* 796. Similar results are obtained for dendrimers **2** and **3**. Dendrimer **3** is a special case due to the two arylsulfonyl groups differently substituted with either methoxyl or cyano groups in the *para* position. In its MALDI mass spectrum, peaks at *m/z* 967 ($\Delta m = 165$), 822 ($\Delta m = 330 = 2 \times 165$), and 657 ($\Delta m = 495 = 3 \times 165$) are seen, all of them accompanied by sodium and potassium adducts. In addition, a signal appears at *m/z* 786 ($\Delta m = 366$) without the corresponding adducts. Consequently, we observe a regular pattern which can be correlated with the loss of arylsulfonyl groups, which in the case of **1** have a mass of 171 Da, and of 166 Da for preferential loss of the cyano-substituted arylsulfonyl groups from **3** (note that only minor signals for losses of the methoxy-substituted arylsulfonyl groups from **3** are observed). The difference of 1 Da between the molecular mass of one of these terminal branches and the observed mass differences is due to a proton at the remaining sulfonamide nitrogen atom which replaces the arylsulfonyl group. The presence of these protons and the observation of the alkali ion adducts suggest that the arylsulfonyl groups are lost before the transition of the ions into the highly diluted gas phase. In contrast, the signals at *m/z* 796 (**1**) and *m/z* 786 (**3**) correspond to fragmentations occurring in the gas phase after ionization. This assumption is confirmed by the MS/MS experiments discussed below. Thus, the ESI mass spectra confirm the absence of incompletely substituted dendrimers (except for small contributions of **6**–**8** when synthesis-grade TREN is used). In marked contrast, signals are observed in the MALDI mass spectra which, without the purity information coming from the ESI mass spectra, could easily be misinterpreted as incompletely substituted defect variants of the desired dendrimers. Consequently, a more in-depth mass spectrometric study employing different ionization techniques is indicated in cases where the MALDI mass spectra point to the presence of large amounts of defects, because they may be formed during laser irradiation.

It is well known that sulfonamides can be used as photocleavable protective groups for amino groups.[13] Usually, the wavelength of the light required for deprotection is in the UV range (254 nm),[14] far below the wavelength of the N_2

laser of our MALDI instrument (337 nm). To exclude induction of such a photochemical reaction by the MALDI laser, UV spectra of the dendrimers were recorded (Figure 2). They all show hardly any absorption around 337 nm and

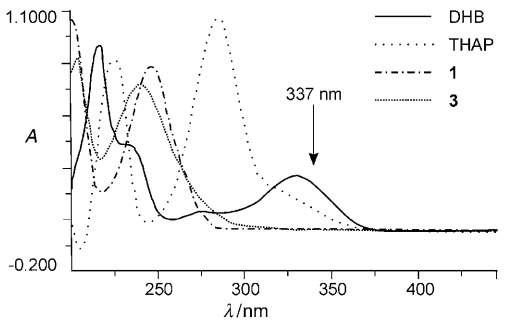

Figure 2. UV spectra of two matrices and dendrimers **1** and **3**, each dissolved in methanol at a concentration of 0.1 mg/10 mL. Clearly, the matrices show absorption bands at the wavelength of the MALDI laser (337 nm), which is not the case for the dendrimers. A = absorbance.

thus should not absorb light energy from the MALDI laser. Furthermore, 2,5-dihydroxybenzoic acid has a strong absorption in this region, so that a photochemical cleavage of the S–N bonds of the dendrimers can be safely ruled out. This is in line with an attempt to ionize the dendrimers with laser desorption/ionization (LDI) in the absence of a matrix. No signals for dendrimer ions were observed, in line with the fact that the light energy of the laser is not efficiently absorbed. This contrasts with an earlier literature report[15] on a different type of dendrimer, which suggested that bond cleavages in the branches of dendrimers are due to photochemical reactions. For the dendrimers studied here, we conclude that a thermal reaction with the matrix occurs.

A reasonable mechanism which accounts for these thermal reactions during the MALDI process is shown in Scheme 2. In the acidic matrix, protonation at a sulfonimide

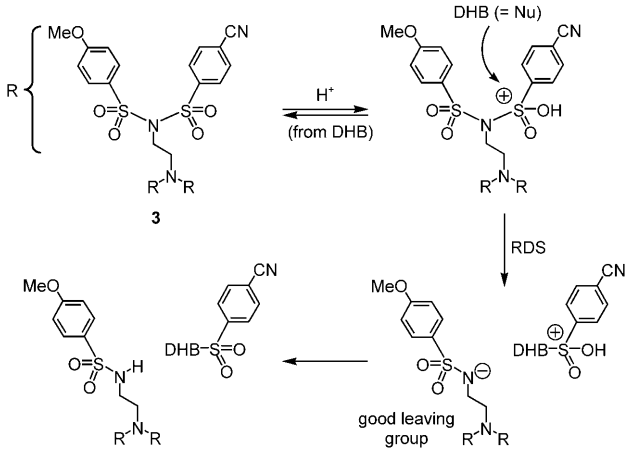

Scheme 2. Mechanism which rationalizes the observed fragmentations of the dendrimers during the MALDI process in terms of a thermal reaction with the 2,5-dihydroxybenzoic acid (DHB) matrix. RDS = rate-determining step.

group occurs to some extent followed by attack of a matrix molecule acting as a nucleophile. The remaining sulfonamide anion is well stabilized by conjugation with the adjacent sulfonyl group and finally is protonated. In view of the rather high temperatures reached in the sample by laser irradiation, this reaction may become fast enough to compete efficiently with desorption of the analyte from the matrix. The proposed mechanism is also in line with the observation of almost exclusive cleavage of the cyano-substituted arylsulfonyl groups in **3**. Electron-withdrawing substituents like the cyano group help to increase the electrophilicity at the SO_2 group and thus favor nucleophilic attack in the rate-determining step, while electron-donating substituents such as methoxy decrease it and thus hamper the reaction. Other matrices were tested, and the results are discussed below in the context of the second-generation dendrimers.

First-generation TREN-based persulfonylated dendrimers: Tandem-MS experiments:[16] ESI-generated protonated parent ions of intact dendrimers **1**–**3** were isolated as their monoisotopic ions in the cell of the Fourier-transform ion-cyclotron-resonance (FT-ICR) mass spectrometer. Subsequently, collisions with argon as the collision gas induced fragmentation. The collision-induced decay (CID) spectra show a series of fragmentation products (Figure 3), which can be categorized into four classes (A–D), as shown in Scheme 3 for protonated **1**. These four reactions are common to all three dendrimers irrespective of their substitution with methoxy or cyano groups at the periphery. All four primary fragments are followed by successive losses of terminal arylsulfonyl branches (dotted arrows in Figure 3), generated by S–N bond cleavages ($\Delta m = 171$ for **1** and **3** and minor contributions of $\Delta m = 166$ for **3**). Note that no fragment ion is observed at the m/z values for cleaved branches that were observed in the MALDI mass spectra, and this confirms that these MALDI-induced processes are not gas-phase reactions, but occur during ionization in the matrix.

Fragmentation pathway A corresponds to a favorable 1,2-elimination reaction at one of the six branches. The fact that fragmentation channel A leads predominantly to the loss of the methoxyl-substituted arylsulfonyl group for protonated **3** rather than the cyano-substituted one underlines that the gas-phase fragmentation pathways significantly differ from the reaction observed in the matrix, where the cyano-substituted branches were cleaved with high preference. Pathway B is only a very minor reaction channel and represents a 1,2-elimination reaction within the TREN scaffold. The most intense fragment in the CID spectrum of $[\mathbf{1}+H]^+$ is due to channel C, in which an immonium ion is formed as the product. It is this fragment which also appears in the MALDI mass spectra, unaccompanied by any sodium or potassium adduct. Thus, these signals in the MALDI mass spectrum were assigned to a real gas-phase reaction rather than a thermal reaction in the matrix. Finally, in pathway D, the protonated, central tertiary amine acts as a leaving group. A stable ionic product can easily be formed through

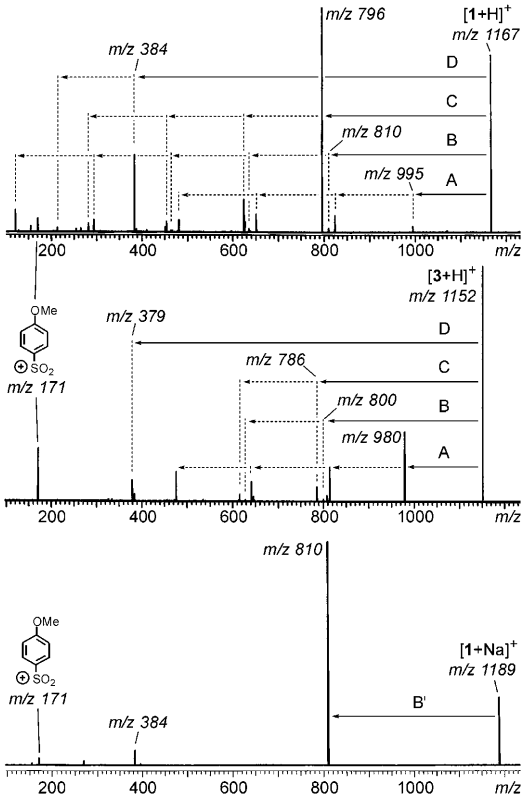

Figure 3. Collision-induced decay (CID) spectra of mass-selected protonated dendrimer ions $[\mathbf{1}+H]^+$ (top) and $[\mathbf{3}+H]^+$ (center). Bottom: For comparison, the CID spectrum of the mass-selected sodium adduct $[\mathbf{1}+Na]^+$ is shown. Labels A–D and B′ refer to the reaction mechanisms depicted in Schemes 3 and 4; dotted arrows represent consecutive losses of arylsulfonyl branches.

a Wagner–Meerwein-type 1,2-hydride shift, which generates a resonance-stabilized cation at *m/z* 384 (for **1**) and *m/z* 379 (for **3**). All fragmentation mechanisms are in agreement with the assumption of protonation of the dendrimer at the most basic site, which is certainly the central tertiary amine.

Much cleaner CID spectra are obtained when the sodium adducts $[\mathbf{1}+Na]^+$–$[\mathbf{3}+Na]^+$ or their potassium analogues are subjected to collisional activation. As a representative example, the spectrum obtained for $[\mathbf{1}+Na]^+$ is shown at the bottom of Figure 3. Besides two minor fragments at *m/z* 171 (the arylsulfonyl cation) and at *m/z* 384 (the product of channel D in Scheme 3), only one major product is observed at *m/z* 810, which can be attributed to a reaction analogous to channel B and is therefore denoted B′ (Scheme 4). It becomes clear now why no Na^+ and K^+ adducts accompany the ion at *m/z* 796 observed in the MALDI mass spectrum of **1**. While decomposition of $[\mathbf{1}+H]^+$ in the gas phase yields this ion with high abundance (Figure 3, top), the alkali metal adducts do not induce the same reaction. The large difference in the CID spectra of the protonated dendrimers as compared to the sodium adducts can easily be understood by assuming different locations for the charge. While protonation occurs at the central tertiary amine nitrogen atom, the alkali metal ions rather bind to the periphery, as shown in Scheme 4. This assignment is in line with the finding that impurities such as **6** do not appear in the ESI mass spectrum as protonated ions, but preferentially bind Na^+ or K^+ (Figure 1). These impurities do not bear any amine nitrogen atom and thus do not have a position where they can easily be protonated. Instead, the intact dendrimer

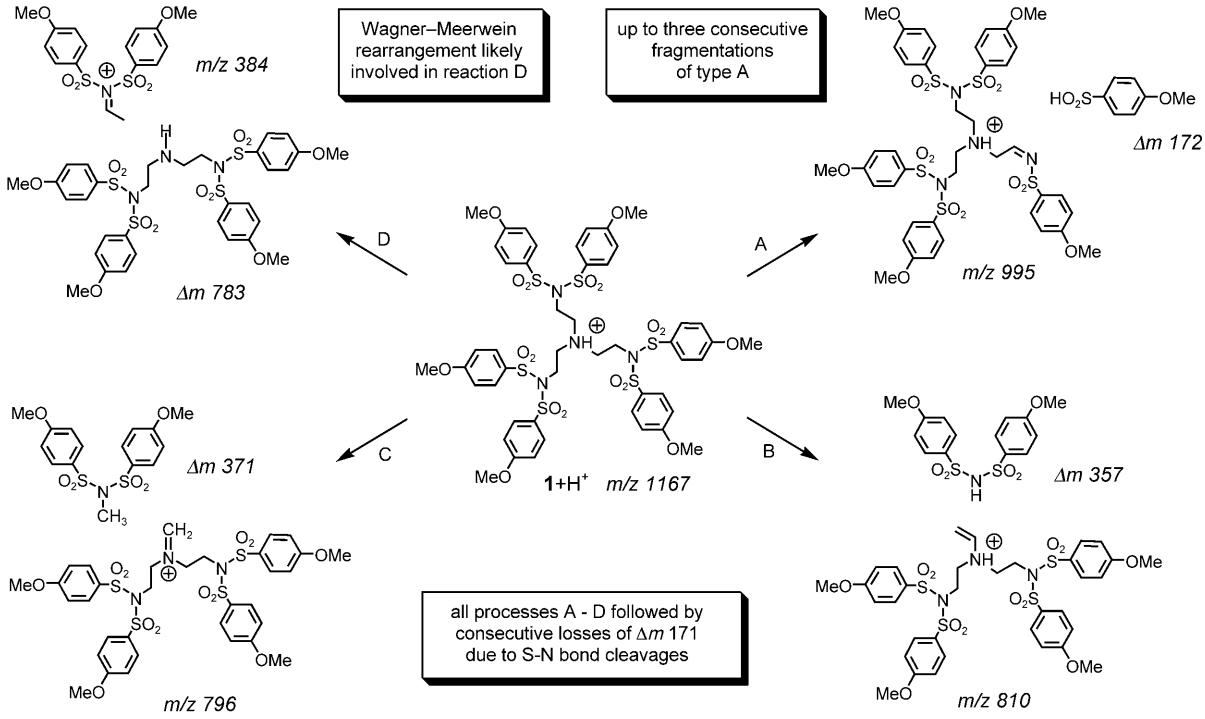

Scheme 3. Fragmentation reactions of $[\mathbf{1}+H]^+$ as observed in the CID experiment.

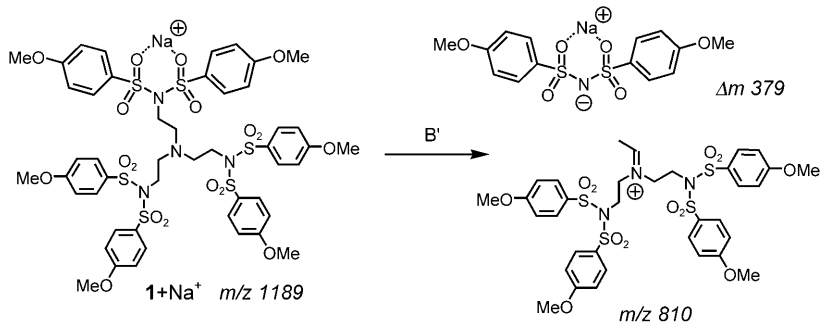

Scheme 4. Most prominent fragmentation reaction of $[\mathbf{1}+\mathrm{Na}]^+$.

with its basic amino nitrogen atom generates much more abundant proton than alkali metal adducts.

Second-generation TREN-based persulfonylated dendrimers: The experience with the first-generation dendrimers was confirmed with their second-generation analogues. Figure 4 compares the ESI-FT-ICR mass spectrum (top) and the MALDI-TOF mass spectrum (bottom) of **4** (Scheme 1). Differences between the two ionization methods similar to those of the first-generation dendrimers are observed. However, one difference is remarkable: no more than three branches were cleaved from **1**–**3** irrespective of the laser power used for ionization of these dendrimers. Likely, only one arylsulfonyl group can thus be removed from each of the three sulfonimides. This is different for both second-generation dendrimers **4** and **5**, for both of which up to nine missing branches could be detected. Due to the rather low signal-to-noise ratio, we were unable to detect more than that, but it seems reasonable to extrapolate that all twelve peripheral sulfonyl groups could finally be removed. In marked contrast, no cleavage was observed at the interior sulfonamide groups. These findings can be rationalized by considering the stability of the leaving group according to the mechanism depicted in Scheme 2.

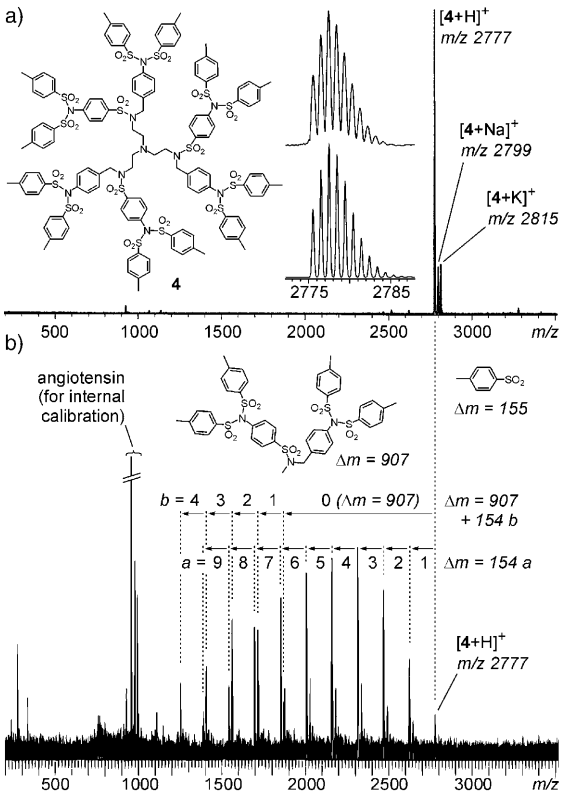

Figure 4. a) ESI-FT-ICR mass spectrum of a 50 μM solution of **4** in methanol with 1% acetic acid added. The inset shows the experimental (top) and the calculated (bottom) isotope patterns. b) MALDI-TOF mass spectrum of **4** with DHB as matrix. Signals of angiotensin, which was used for internal calibration, are visible between 900 and 1000 Da.

In the case of **1**–**3**, the N-centered anion is stabilized through conjugation with the second sulfonyl group. Cleavage of the second S–N bond would leave an unstabilized N-centered anion and thus does not occur. For **4** and **5**, the situation is similar as far as the first sulfonyl group is concerned. Breaking the second S–N bond leads to an anion which can be stabilized by conjugation with the adjacent aromatic ring. Consequently, this reaction is feasible. Cleavage of the inner sulfonamides again gives rise to an anion that is not stabilized by conjugation and thus does not occur. Furthermore, these sulfonamides are buried inside the dendrimer structure and thus are likely shielded against reactions with the matrix by steric hindrance of the peripheral branches. One conclusion from these findings is that the MALDI mass spectra provide some information about the number of sulfonimide groups for dendrimers in which the third substituent at the imide nitrogen atom is an alkyl group.

A second series of signals is found for $\Delta m = 907 + 154\,b$, where $b = 1$–4 (Figure 4). As was found for the G1 dendrimers **1**–**3**, the signals in this series are not accompanied by sodium and potassium adducts. Consequently, they can be attributed to a gas-phase reaction of the protonated species following ionization. Figure 4 shows the fragment corresponding to a loss of 907 Da. According to the categorization in Scheme 3, it is formed by fragmentation pathway C. The mass difference is, of course higher, because of the larger dendron size. CID experiments with protonated $[\mathbf{4}+\mathrm{H}]^+$ reveal the loss of 907 Da to correspond to one of the major fragmentation products. Dendrimer **5** exhibits an analogous behavior, so we refrain from an in-depth discussion here.

Other matrices were tested,[17] that is, 2,4,6-trihydroxyacetophenone (THAP), 1,8,9-trihydroxyanthracene (dithranol), 3-β-indole acrylic acid (IAA), 9-nitroanthracene (9-NA), and 2-[(2*E*)-3-(4-*tert*-butylphenyl)-2-methylprop-2-enylidene]malononitrile (DCTB)[18] (Figure 5). Whereas THAP yielded only very noisy spectra with hardly visible signals

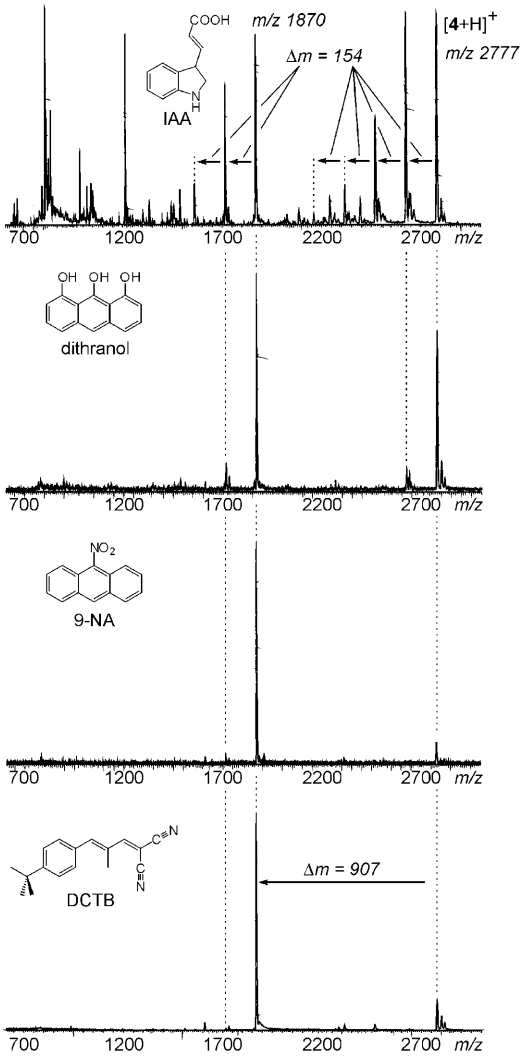

Figure 5. MALDI mass spectra of **4** in different matrices, obtained under the same conditions. From top to bottom: IAA, dithranol, 9-NA, DCTB.

for the dendrimers, the other matrices nicely permitted the ionization of **1**–**5** (Figure 5). Depending on the acidity of the matrix, different abundances of cleavage products are observed. IAA, which is a carboxylic acid like DHB, shows a reduced, but still significant number of sulfonyl group losses. Dithranol with its less acidic phenolic OH groups yields quite a clean spectrum which contains only minor signals for the decomposition products. In the MALDI mass spectra obtained with aprotic matrices such as 9-NA and DCTB, significant cleavage products are no longer observed. Instead, the intensity of the gas-phase process corresponding to $\Delta m = 907$ (Figure 4) increases. One advantage of DCTB over 9-NA is the much lower laser power necessary to generate sufficiently high signal intensities for high-quality mass spectra. These findings, in particular, the dependence of the extent of dendrimer–matrix reactions on the acidity of the matrix, support the mechanism for the thermal reaction of the dendrimers with matrix molecules as discussed above (Scheme 2).

POPAM-based persulfonylated dendrimers: A second series of dendrimers was investigated which are based on a polypropyleneamino (POPAM) scaffold. While the synthesis of structurally perfect persulfonylated G1 POPAM dendrimers **9** is possible, the G2 analogue **16** could not be obtained (Scheme 5).[12b] In the synthesis of **9**, several defect variants were formed some of which (**10**–**15**) could be isolated for a mass spectrometric investigation. All attempts to prepare **16** yielded only products corresponding to half a POPAM scaffold (**17**-Cl, **18**) or defects thereof (**19**). Although the unsuccessful synthesis of higher generation persulfonylated dendrimers is certainly a drawback, these molecules are highly interesting targets in the context of the present MS study, because they allow us to differentiate different defects by mass spectrometric means.

The ESI mass spectrum (Figure 6) of **17**-Cl serves as an example. Although it is not as clean as those obtained for **1**–**5**, it shows a prominent signal for $\mathbf{17}^+$, the experimental isotope pattern of which is in excellent agreement with the calculated one. The MALDI-TOF mass spectrum (DHB matrix) again exhibits the parent ion $\mathbf{17}^+$ and a series of up to four losses of sulfonyl groups, presumably one from each sulfonimide group. These signals are not seen in the ESI mass spectra, except for a small signal for the loss of the first sulfonyl group. Consequently, the same pattern and the same differences between ESI and MALDI mass spectrometry are found as obtained for **1**–**5**.

More interestingly, the CID mass spectra of POPAM-based **9**–**15** (Figure 7) permit the type of defects present in the molecules to be identified. Structurally perfect **9** undergoes only one fragmentation reaction and follows a mechanism earlier described by Meijer et al. for unsubstituted POPAM dendrimers (Scheme 6).[9a] Protonation at one of the central tertiary amino groups generates a good leaving group. The second tertiary amine attacks the carbon atom adjacent to the protonated amine and generates the fragment at *m/z* 802 by formation of a five-membered ring (Figure 7a). This reaction is energetically favorable and also occurs for the defect variants **10**–**12**. If one sulfonyl group is missing, the dendrimer is no longer symmetrically substituted and thus fragmentation generates two different products at *m/z* 648 and 802 (Figure 7b). For this defect (**10**), only one possible isomer can be generated. This is different if two branches are missing. Two isobaric isomers with the same elemental composition can be formed, one with one defect on each of the two dendrimer halves (**11**) and another one which has both defects on the same side (**12**). Indeed, the fraction obtained after column chromatography containing dendrimers with a molecular mass of 1240 Da contained both isomers. While this cannot be deduced from the ESI or MALDI mass spectra alone, the CID spectrum of mass-selected $[\mathbf{11}+\mathrm{H}]^+$ and $[\mathbf{12}+\mathrm{H}]^+$ (Figure 7c) exhibits three fragments. The ion at *m/z* 648 cannot be formed from $[\mathbf{12}+\mathrm{H}]^+$ and thus must be due to the presence of **11** in the sample. Vice versa, the two ions at *m/z* 494 and *m/z* 802 cannot be formed from $[\mathbf{11}+\mathrm{H}]^+$ and therefore are generated in the fragmentation of protonated **12**.

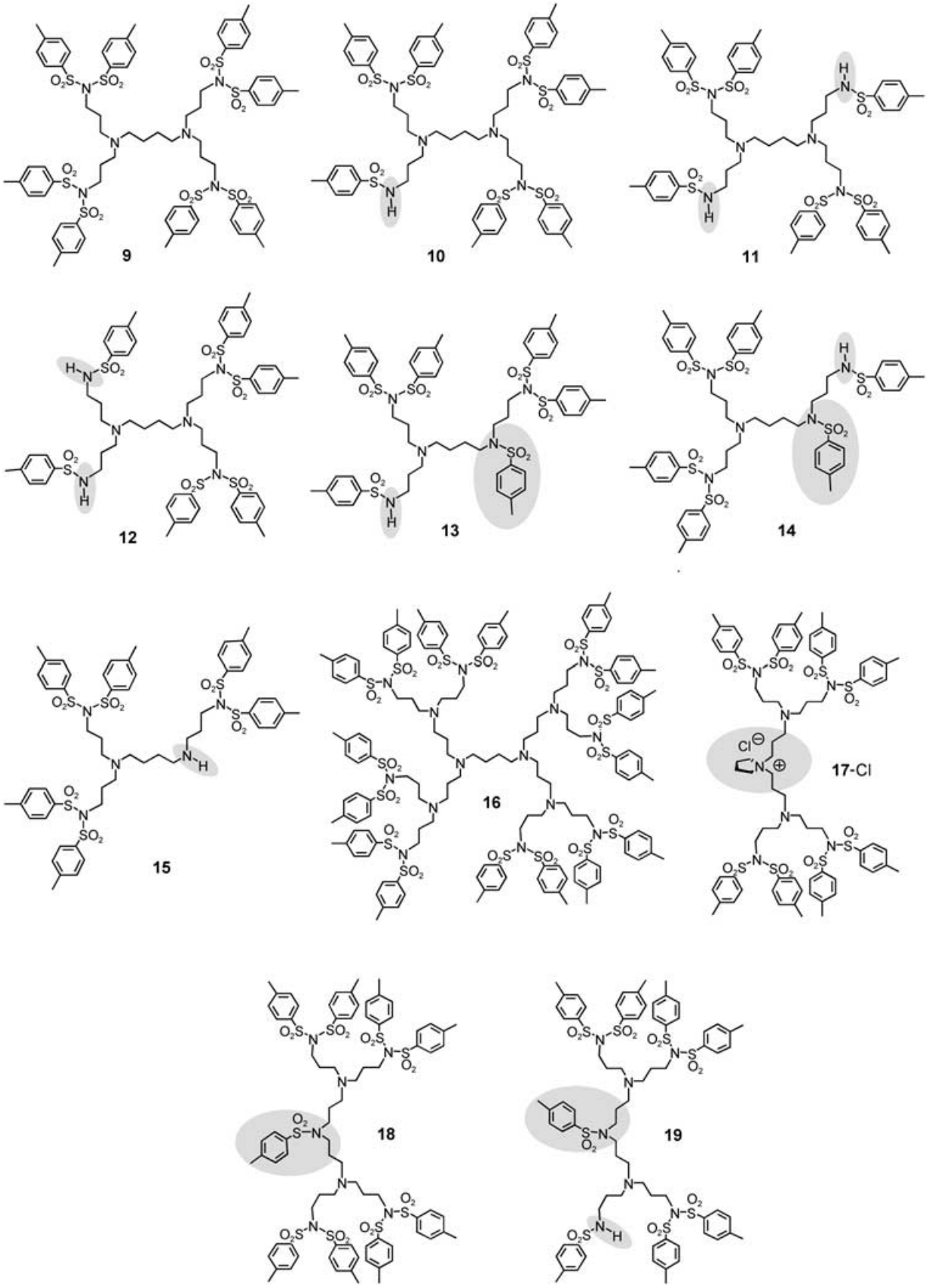

Scheme 5. Persulfonylated G1 POPAM dendrimer **9** and defect variants **10**–**15**, which were isolated during the synthesis (top). Persulfonylated G2 POPAM dendrimer **16**, which could not be obtained, and defects **17**–**19** formed during the synthesis (bottom).

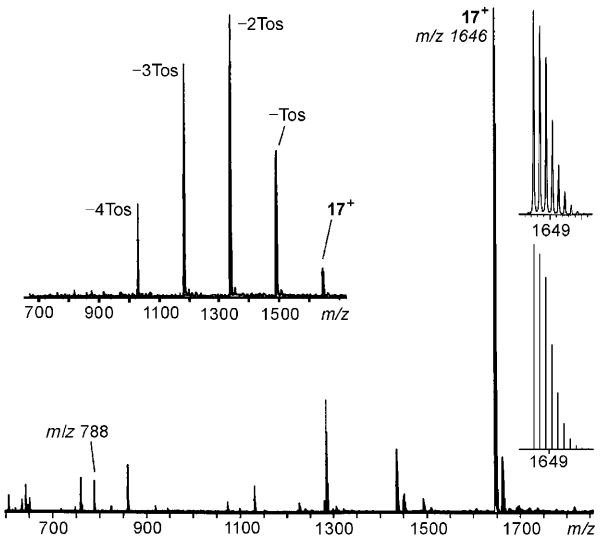

Figure 6. ESI-FT-ICR mass spectrum of $\mathbf{17}^{+}Cl^{-}$. The insets on the right show the experimental and calculated isotope patterns. The left inset shows the corresponding MALDI mass spectrum with DHB as matrix.

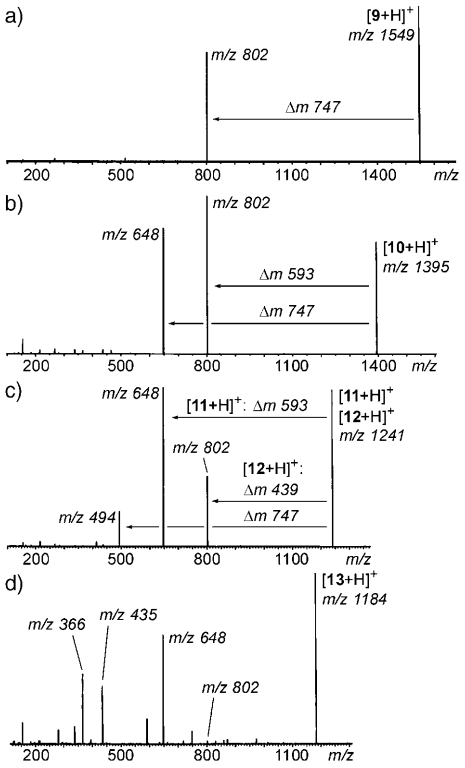

Figure 7. CID spectra of mass-selected (from top to bottom) $[\mathbf{9}+H]^{+}$, $[\mathbf{10}+H]^{+}$, a mixture of isobaric $[\mathbf{11}+H]^{+}$ and $[\mathbf{12}+H]^{+}$, and $[\mathbf{13}+H]^{+}$.

The situation becomes more complex for the other type of defect, as realized in **13**–**15**. While the G1 POPAM scaffold is intact in **10**–**12**, one of the four propyleneamine branches is missing in **13**–**15**. Defect **15** can be expected to follow the mechanism depicted in Scheme 6. In the CID spectrum (Figure 7d) of a sample containing a defect dendrimer with the corresponding mass of 1184 Da, only very minor signals appear for the two expected fragmentation products at *m/z* 802 and 437. Consequently, **15** can be ruled out as the major component in this sample. The other two isomers **13** and **14** both bear a sulfonyl group at the defect position in the POPAM scaffold. Consequently, the fragmentation reaction shown in Scheme 6 cannot take place easily, although its products are still observed in the CID spectra. The higher barrier for this reaction is expressed in the much more complex CID spectrum in Figure 7d, which shows that other fragmentation processes can now compete. The fragmentations can all be analyzed in terms of the reactions discussed so far for **1**–**9**. Nevertheless, a fragment at *m/z* 648 is observed which was found already for **10**. This fragment clearly indicates that isomer **13** is the major component in the sample. Contributions of **14** would instead lead to a fragment at *m/z* 802, which is low in intensity.

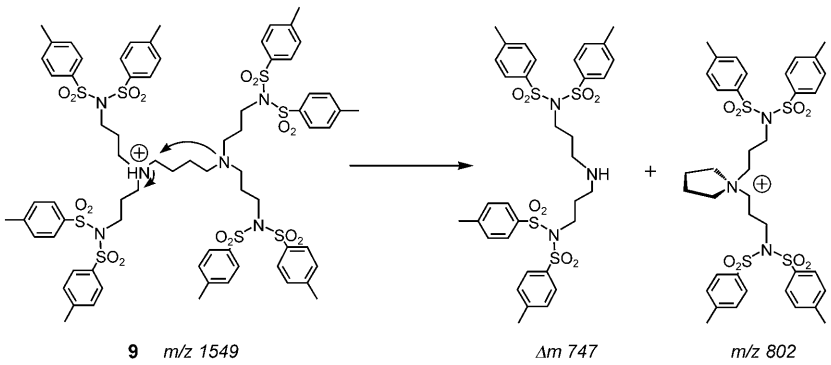

Scheme 6. Fragmentations mechanism of POPAM-based persulfonylated G1 dendrimer **9**.

The CID mass spectra of $\mathbf{17}^{+}$ and protonated **18** and **19** are shown in Figure 8. All of them are cleavage products formed during the attempted synthesis of **16**. The cleavage occurs in the central butylenediamine moiety and has been discussed before.[12b] Compounds **17**-Cl and **18** are the two fully substituted cleavage products, while **19** bears an additional defect in the periphery. The charge in $\mathbf{17}^{+}$ is located at the central, quaternary ammonium nitrogen atom and unlike a proton cannot easily move within the dendrimer structure. This position is blocked in **18** and **19** by a sulfonyl group, so that these two molecules are likely protonated at one of the two tertiary amines rather than the central nitrogen atom.

These differences in the location of the charge are reflected in the CID mass spectra (Figure 8). Cation $\mathbf{17}^{+}$ loses one complete branch including the five-membered ring with the ammonium nitrogen atom ($\Delta m = 858$) to yield a cation that corresponds to the second branch (*m/z* 788). This reaction

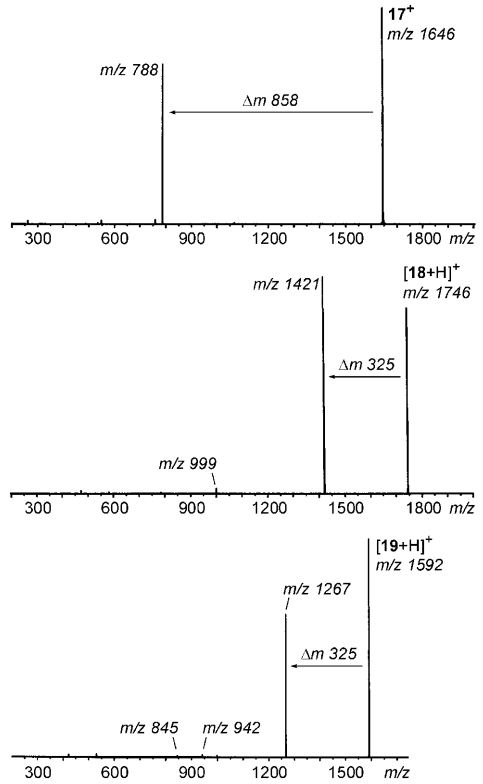

Figure 8. CID mass spectra of mass-selected, monoisotopic $\mathbf{17}^{+}Cl^{-}$ (top), $[\mathbf{18}+H]^{+}$ (center), and $[\mathbf{19}+H]^{+}$ (bottom).

again is facilitated by the quaternary ammonium cation, which is a good leaving group. No other intense signals are observed, because the charge cannot easily move to another location. In contrast, protonated **18** and **19** both exhibit an intense loss of $\Delta m = 325$, which corresponds to a proton transfer from the tertiary amine to one of the sulfonimide groups followed by loss of that sulfonimide unit.

Finally, Figure 9 depicts the CID spectra for the mass-selected potassium adducts of **9** and **10**. Again, a fragmentation analogous to channel B′ in Scheme 4 is most prominent and points to the location of the potassium ion at the sulfonamide group, as discussed above. Still, the structure-sensitive fragmentations at *m/z* 648 and 802 can be observed, so that the alkali metal ion adducts also permit the structural features of the defect dendrimers to be examined. Consequently, the fragmentation reactions observed in the CID mass spectra of protonated or alkali-cationized dendrimer defect variants are quite sensitive even to subtle changes in the structure and thus provide much more information on the nature of defects than the ESI or MALDI mass spectra alone.

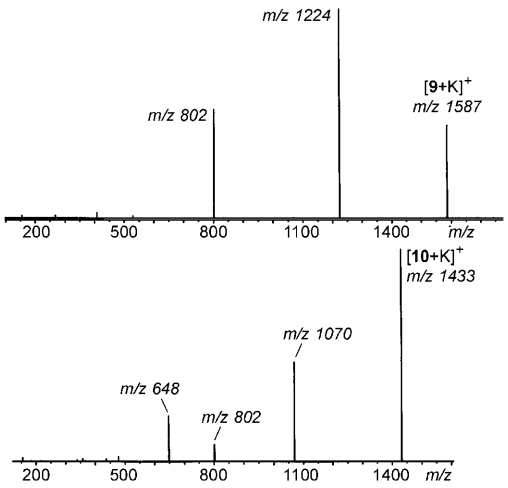

Figure 9. CID mass spectra of mass-selected, monoisotopic $[\mathbf{9}+K]^{+}$ (top) and $[\mathbf{10}+K]^{+}$ (bottom).

Conclusions

One of the central conclusions of this study is that MALDI mass spectrometry, which has long-been considered to be a precise and reliable tool for the characterization of dendrimers, may lead to false negative results. To the best of our knowledge, we for the first time report examples of dendrimers which generate fragments in the MALDI process identical to those expected as defects from an incomplete substitution reaction during dendrimer synthesis. This result may be of importance to synthetic chemists working in the dendrimer field. In those cases in which MALDI gives rise to spectra that appear to indicate large amount of defects, it is recommended to double-check the result by ESI mass spectrometry or the use of a variety of different matrices.

Beyond that, tandem MS experiments provide a means to distinguish different defect variants. At least for the smaller dendrimers discussed here, different defects leading to structures with the same elemental composition can be identified. With an understanding of the fragmentation mechanisms, such a differentiation is even possible from raw products by first mass-selecting one of the defect ions and then subjecting it to an MS/MS experiment to analyze its structure and to identify whether it exists as a mixture of isobaric isomers. Tandem mass spectrometry thus provides more detailed structural information than simple mass spectra. The large differences in the fragmentation patterns of protonated and alkali-metal-cationized ions indicate that the sites where the charge is located are likely different.

Experimental Section

Synthesis: All dendrimers were synthesized and characterized according to recently published procedures.[12]

MALDI mass spectrometry: MALDI mass spectra were recorded on a Micromass MALDI-TofSpec E mass spectrometer equipped with an N_2 laser (337 nm). All matrices were used as purchased and applied in an 800-fold molar excess relative to the analyte. Matrices and samples (0.5 mg) were dissolved in 400 μL of $CHCl_3$/MeOH (3/1). Then, 1 μL of the mixture was pipetted onto the stainless steel MALDI target. The matrix crystallized in a small spot of about 3 mm diameter upon evaporation of the solvent in a stream of air.

ESI mass spectrometry: ESI mass spectra and MS/MS spectra were recorded on a Bruker APEX IV Fourier transform ion-cyclotron-resonance (FT-ICR) mass spectrometer with an Apollo electrospray ion source equipped with an off-axis 70° spray needle. Typically, methanol with 1% of acetic acid served as the spray solvent, and 50 μM solutions of the analytes were used. Analyte solutions were introduced into the ion source with a syringe pump (Cole-Parmers Instruments, Series 74900) at flow rates of about 3–4 $\mu L\,min^{-1}$. Ion transfer into the first of three differential pumping stages occurred through a glass capillary with 0.5 mm inner diameter and nickel coatings at both ends. Ionization parameters were adjusted as follows: capillary voltage: −4.7 to −4.9 kV; end plate voltage: −4.2 to −4.5 kV; cap exit voltage: +200 to +300 V; skimmer voltages: +8 to +12 V; temperature of drying gas: 100 °C. The flows of the drying and nebulizer gases were kept in a medium range (ca. 10 psi). The ions were accumulated in the instruments hexapole for 2–3 s, introduced into the FT-ICR cell, which was operated at pressures below 10^{-10} mbar, and detected by a standard excitation and detection sequence. For each measurement, 16–64 scans were averaged to improve the signal-to-noise ratio.

For MS/MS experiments, the whole isotope pattern of the ion of interest was isolated by applying correlated sweeps, followed by shots to remove the higher isotopologues. After isolation, argon was introduced into the ICR cell as collision gas through a pulsed valve at a pressure of about 10^{-8} mbar. The ions were accelerated by a standard excitation protocol and detected after 2 s pumping delay. A sequence of several different spectra was recorded at different excitation pulse attenuations to get at least a rough and qualitative idea of the effects of different collision energies on the fragmentation patterns.

Acknowledgements

We are grateful to Prof. Fritz Vögtle (Bonn) for his advice and continuous support and thank Dr. Heinrich Luftmann (Münster) for providing us with a sample of the DCTB matrix. This work was funded by the Deutsche Forschungsgemeinschaft (DFG) and the Fonds der Chemischen Industrie (FCI). C.A.S. thanks both institutions for a Heisenberg fellowship (DFG) and a Dozentenstipendium (FCI).

[1] E. Buhleier, W. Wehner, F. Vögtle, *Synthesis* **1978**, 155–158.

[2] a) C. G. Juo, L. L. Shiu, C. K. F. Shen, T. Y. Luh, G. R. Her, *Rapid Commun. Mass Spectrom.* **1995**, *9*, 604; b) G. Coullerez, H. J. Mathieu, S. Lundmark, M. Malkoch, H. Magnusson, A. Hult, *Surf. Interface Anal.* **2003**, *35*, 682–692.

[3] The earliest reports available after the initial article by Vögtle et al.: a) D. A. Tomalia, H. Baker, J. R. Dewald, M. Hall, G. Kallos, S. Martin, J. Roeck, J. Ryder, P. Smith, *Polym. J.* **1985**, *17*, 117–132; b) G. R. Newkome, Z.-Q. Yao, G. R. Baker, V. K. Gupta, *J. Org. Chem.* **1985**, *50*, 2003–2004.

[4] For recent reviews, see a) F. Zeng, S. C. Zimmerman, *Chem. Rev.* **1997**, *97*, 1681–1712; b) A. Archut, F. Vögtle, *Chem. Soc. Rev.* **1998**, *27*, 233–240; c) D. K. Smith, F. Diederich, *Chem. Eur. J.* **1998**, *4*, 1351–1361; d) M. Fischer, F. Vögtle, *Angew. Chem.* **1999**, *111*, 934–955; *Angew. Chem. Int. Ed.* **1999**, *38*, 884–905; e) A. W. Bosman, H. M. Jansen, E. W. Meijer, *Chem. Rev.* **1999**, *99*, 1665–1688; f) G. R. Newkome, E. He, C. N. Moorefield, *Chem. Rev.* **1999**, *99*, 1689–1746; g) J.-F. Nierengarten, *Chem. Eur. J.* **2000**, *6*, 3667–3670; h) A. D. Schlüter, J. P. Rabe, *Angew. Chem.* **2000**, *112*, 860–880; *Angew. Chem. Int. Ed.* **2000**, *39*, 864–883; i) G. R. Newkome, C. N. Moorefield, F. Vögtle, *Dendrimers and Dendrons. Concepts, Syntheses, Applications*, Wiley-VCH, Weinheim, Germany, **2001**; j) R. Haag, *Chem. Eur. J.* **2001**, *7*, 327–335; k) S. Hecht, J. M. J. Fréchet, *Angew. Chem.* **2001**, *113*, 76–94; *Angew. Chem. Int. Ed.* **2001**, *40*, 74–91; l) J. M. J. Fréchet, D. A. Tomalia, *Dendrimers and Other Dendritic Polymers*, Wiley, New York, **2001**; m) S. M. G. Grayson, J. M. J. Fréchet, *Chem. Rev.* **2001**, *101*, 3819–3868.

[5] See, for example, a) T. Kawaguchi, K. L. Walker, C. L. Wilkins, J. S. Moore, *J. Am. Chem. Soc.* **1995**, *117*, 2159–2165; b) B. L. Schwartz, A. L. Rockwood, R. D. Smith, D. A. Tomalia, R. Spindler, *Rapid Commun. Mass Spectrom.* **1995**, *9*, 1552; c) J. W. Leon, M. Kawa, J. M. J. Fréchet, *J. Am. Chem. Soc.* **1996**, *118*, 8847–8859; d) M. S. Wendland, S. C. Zimmerman, *J. Am. Chem. Soc.* **1999**, *121*, 1389–1390; e) P. B. Rheiner, D. Seebach, *Chem. Eur. J.* **1999**, *5*, 3221–3236; f) L. Bu, W. K. Nonidez, J. W. Mays, N. B. Tan, *Macromolecules*, **2000**, *33*, 4445–4452; g) L. Zhou, D. H. Russell, M. Zhao, R. M. Crooks, *Macromolecules* **2001**, *34*, 3567–3573; h) H. Chen, M. He, X. Cao, X. Zhou, J. Pei, *Rapid Commun. Mass Spectrom.* **2004**, *18*, 367–370.

[6] Selected examples: a) G. J. Kallos, D. A. Tomalia, D. M. Hedstrand, S. Lewis, J. Zhou, *Rap. Commun. Mass Spectrom.* **1991**, *5*, 383–386; b) J. C. Hummelen, J. L. J. van Dongen, E. W. Meijer, *Chem. Eur. J.* **1997**, *3*, 1489–1493; c) L. P. Tolic, G. A. Anderson, R. D. Smith, H. M. Brothers II, R. Spindler, D. A. Tomalia, *Int. J. Mass Spectrom.* **1997**, *165/166*, 405–418; d) U. Puapaiboon, R. T. Taylor, *Rapid Commun. Mass Spectrom.* **1999**, *13*, 508–515; e) S. Watanabe, M. Sato, S. Sakamoto, K. Yamaguchi, M. Iwamura, *J. Am. Chem. Soc.* **2000**, *122*, 12588–12589; f) S. M. Cohen, S. Petoud, K. N. Raymond, *Chem. Eur. J.* **2001**, *7*, 272–279; g) Y. Rio, G. Accorsi, H. Nierengarten, J.-L. Rehspringer, B. Hönerlage, G. Kopitkovas, A. Chugreev, A. Van Dorsselaer, N. Armaroli, J.-F. Nierengarten, *New J. Chem.* **2002**, *26*, 1146–1154; h) A. T. Iavarone, E. R. Williams, *J. Am. Chem. Soc.* **2003**, *125*, 2319–2327.

[7] Representative examples for the analysis of defects by mass spectrometry: a) M. Liu, J. M. J. Fréchet, *Polym. Bull.* **1999**, *43*, 379–386; b) E. K. Wolter, M. J. Cloninger, *Org. Lett.* **2002**, *4*, 7–10; c) G. D. Engel, L. H. Gade, *Chem. Eur. J.* **2002**, *8*, 4319–4329; d) W. Zhang, S. E. Tichy, L. M. Pérez, G. C. Maria, P. A. Lindahl, E. E. Simaneck, *J. Am. Chem. Soc.* **2003**, *125*, 5086–5094; e) S. C. Zimmerman, I. Zharov, M. S. Wendland, N. A. Rakow, K. S. Suslick, *J. Am. Chem. Soc.* **2003**, *125*, 13504–13518; f) A. Dirksen, U. Hahn, F. Schwanke, M. Nieger, J. N. H. Reek, F. Vögtle, L. De Cola, *Chem. Eur. J.* **2004**, *10*, 2036–2047.

[8] See, for example, a) U. Puapaiboon, R. T. Taylor, J. Jai-nhuknan, *Rapid Commun. Mass Spectrom.* **1999**, *13*, 516–520; b) S. Koster, M. C. Duursma, X. Guo, R. A. T. M. Benthem, C. G. de Koster, J. J. Boon, R. M. A. Heeren, *J. Mass Spectrom.* **2002**, *37*, 792–802; c) A. Adhiya, C. Wesdemiotis, *Int. J. Mass Spectrom.* **2002**, *214*, 75–88; d) H. Neubert, K. A. Knights, Y. R. de Miguel, D. A. Cowan, *Macromolecules* **2003**, *36*, 8297–8303; e) S. Koster, M. C. Duursma, J. J. Boon, R. M. A. Heeren, S. Ingemann, R. A. T. M. van Benthem, C. G. de Koster, *J. Am. Soc. Mass Spectrom.* **2003**, *14*, 332–341; f) M. He, S. A. McLuckey, *Rapid Commun. Mass Spectrom.* **2004**, *18*, 960–972;

[9] J.-W. Weener, J. L. J. van Dongen, E. W. Meijer, *J. Am. Chem. Soc.* **1999**, *121*, 10346–10355;

[10] Some selected examples of MS-detected self-assembly through hydrogen bonding: a) P. S. Corbin, L. J. Lawless, Z. Li, Y. Ma, M. J. Witmer, S. C. Zimmerman, *Proc. Natl. Acad. Sci. USA* **2002**, *99*, 5099–5104; through metal coordination: b) H.-J. van Manen, R. H. Fokkens, N. M. M. Nibbering, F. C. J. M. van Veggel, D. N. Reinhoudt; c) A. Rang, H. T. Baytekin, C. A. Schalley, unpublished results.

[11] a) W. Ong, A. E. Kaifer, *Angew. Chem.* **2003**, *115*, 2214–2217; *Angew. Chem. Int. Ed.* **2003**, *42*, 2164–2167; b) T. Yamada, M. Ge, H. Shinohara, K. Kimura, S. Mashiko, *Chem. Phys. Lett.* **2003**, *379*, 458–465; c) M. A. C. Broeren, J. L. J. van Dongen, M. Pittelkow, J. B. Christensen, M. H. P. van Genderen, E. W. Meijer, *Angew. Chem.* **2004**, *116*, 3541–3646; *Angew. Chem. Int. Ed.* **2004**, *43*, 3557–3562; d) C. A. Schalley, C. Verhaelen, F.-G. Klärner, U. Hahn, F. Vögtle, Angew. Chem. **2005**, *117*, 481–485; *Angew. Chem. Int. Ed.* **2005**, *44*, 477–480.

[12] a) F. Vögtle, H. Fakhrnabavi, O. Lukin, *Org. Lett.* **2004**, *6*, 1075–1078; b) F. Vögtle, H. Fakhrnabavi, O. Lukin, S. Müller, J. Friedhofen, C. A. Schalley, *Eur. J. Org. Chem.* **2004**, 4717–4724.

[13] T. W. Greene, P. G. Wuts, *Protective Groups in Organic Synthesis*, Wiley, Chichester, **1999**.
[14] a) A. Abad, D. Mellier, J. P. Pète, C. Portella, *Tetrahedron Lett.* **1971**, *47*, 4555–4558; b) D. Mellier, J. P. Pète, C. Portella, *Tetrahedron Lett.* **1971**, *47*, 4559–4562; c) W. Yuan, K. Fearon, M. H. Gelb, *J. Org. Chem.* **1989**, *54*, 906–910.
[15] J.-C. Blais, C.-O. Turrin, A.-M. Caminade, J.-P. Majoral, *Anal. Chem.* **2000**, *72*, 5097–5105.
[16] L. Shen, Y. Sha, X. Hong, *Rapid Commun. Mass Spectrom.* **2004**, *18*, 1534–1538.
[17] For earlier reports on matrix effects on dendrimer fragmentation, see a) G. Chessa, A. Scrivanti, R. Seraglia, P. Traldi, *Rapid Commun. Mass Spectrom.* **1998**, *12*, 1533–1537; b) R. Kaneko, Y. Wada, *J. Mass Spectrom.* **2003**, *38*, 526–530; c) U. M. Demelbauer, M. Zehl, A. Plematl, G. Allmaier, A. Rizzi, *Rapid Commun. Mass Spectrom.* **2004**, *18*, 1575.
[18] For references dealing with the use of DCTB as a matrix, see a) C. Siedschlag, H. Luftmann, C. Wolff, J. Mattay, *Tetrahedron* **1999**, *55*, 7805–7818; b) B. Gigante, C. Santos, T. Fonseca, M. J. M. Curto, H. Luftmann, K. Bergander, M. N. Berberan-Santos, *Tetrahedron* **1999**, *55*, 6175–6182; c) L. Ulmer, J. Mattay, H. G Torres-Garcia, H. Luftmann, *Eur. J. Mass Spectrom.* **2000**, *6*, 49–52.

Received: December 2, 2004
Revised: April 14, 2005
Published online: July 20, 2005

